8th International Conference on Photonic Technologies LANE 2014

# Influence of the pulse duration onto the material removal rate and machining quality for different types of Steel

Benjamin Lauer[a],*, Beat Jäggi[a], Beat Neuenschwander[a]

[a]*University of Applied Sciences; Institute for Applied Laser, Photonics and Surface Technologies, Switzerland*

**Abstract**

When high requirements concerning machining quality are demanded, ultra short pulsed lasers with pulse durations from a few 100fs to 10ps may be the tool of choice. For these pulses it is known that the removal rate and machining quality slightly increases with shorter pulse duration. But as cost-effectiveness is also a key factor for a successful transfer of a technology to industrial applications, these systems compete against more cost effective systems with pulse durations from several 10ps to a few ns. It was found in previous work that the removal rate for metals strongly depends on the pulse duration. For steel also the composition and microstructure will influence the ablation processes. A systematic study of the removal rate and the machining quality for different types of steel and for pulse durations of several 100 fs to few ns will be presented.

*Keywords:* pulse duration; removal rate; Steel

## 1. Introduction

Systems with 10 ps or shorter pulses show clear advantages concerning machining quality, heat affected zone, debris etc. as shown by Chichkov et al. (1996), Breitling et al. (2004), Dausinger et al. (2003) and Meijer et al. (2002). But even if the excellent machining quality is one of the key advantages of these systems, it may be more cost effective to use fiber based amplifier technologies without Chirped Pulse Amplification (CPA). The pulse duration of these systems is in the range of several 10 ps, (Pierrot et al. (2011), Kanzelmeyer et al. (2011)). For metals the ablation efficiency significantly drops by about a factor of 5 when the pulse duration is raised from 10 ps

---

\* Corresponding author. Tel.: +41-34-42-64184 .
  *E-mail address:* benjamin.lauer@bfh.ch

to 50 ps as shown by Schmid et al. (2011) and Jäggi et al. (2011), for non metals this drop is less pronounced but still present as shown by Neuenschwander et al. (2011).

Another alternative may be offered by actively Q-switched DPSS with pulse durations in the sub-ns range. But the results of these systems should also be compared with fiber based Q-Switched systems with pulse durations in the short ns-range.

The characteristics of the measured ablation efficiency as a function of the pulse duration implies, that the efficiency could increase when the pulse duration is reduced from $10\,ps$ into the sub ps regime. Results corroborating this belief have been reported by Sallé et al. (1999), Le Harzic et al. (2005) and Lopez et al. (2011).This all encourages the development of fiber based ultra short pulsed systems in the fs-regime which can be driven to high average powers by succeeding amplifier stages; recently more than $1\,kW$ average power with fs – laser pulses were demonstrated (Russbueldt et al. (2010 and 2011)). From this point of view sub – ps systems could to be very attractive for laser micro machining.

In Lauer et al. (2013) the Authors show a difference in ablation rate for different types of steel. Hence it is of interest to have a deeper look at the influence of composition and microstructure of steel. Therefore investigations concerning the removal rate and the machining quality have been done for the pulse durations of 10 ps, 50 ps, and 520 ps at 1064 nm wavelength. Investigations in fs- and ns-regime will be done in near future. All experiments were performed on steel grades which are mainly used in the automotive industry. The following steel grades were used:

- DP-K60/98
- DP-K45/78
- CP-W800
- HX340LAD
- RA-K40/70
- MBW1500
- MBW1900
- MBW1900 cured (hot-formed)

The steels from Lauer et al. (2013) stainless steel 1.4301 and high speed steel 1.3343 in initial and hardened state were examined again.

**Nomenclature**

| | |
|---|---|
| $\phi$ | peakfluence |
| $\phi_{th}$ | threshold fluence |
| $\phi_{opt}$ | fluence of the optimal point of ablation |
| $\delta$ | energy penetration |
| $E_p$ | pulse energy |
| $P_{av}$ | average Power |
| $z_{abl}$ | ablation depth |
| $w_0$ | radius of the laser focus |
| $\dot{V}/P_{av}$ | removal rate |

## 2. Theory

### 2.1. Ablation

For ultra short pulses the heat-transfer process in metals is described with the two temperature model as shown by Momma et al. (1996 and 1997); Nolte et al. (1997), Anisimov and Rethfeld (1997) and Christensen (2007) where the temperatures of the electrons and the lattice are treated separately. The results of the model and the experiments show, that the ablation depth $z_{abl}$ can be written in a first approximation as a function of the fluence $\phi$:

$$z_{abl} = \delta \cdot \ln\left(\frac{\phi}{\phi_{th}}\right) \tag{1}$$

$$\phi = \frac{2 \cdot E_p}{\pi \cdot w_0^2} \tag{2}$$

Frequently two different ablation regimes are reported (Nolte et al. (1997), Anisimov and Rethfeld (1997), Christensen (2007), Mannion (2002)): firstly the low fluence regime where the optical penetration depth dominates and secondly the high fluence regime where the energy transport is dominated by the heat diffusion of the hot electrons. Neuenschwander et al. (2012) show that for a top hat beam the efficiency of the ablation process depends on the ratio between the threshold fluence and the applied fluence $\phi_{th}/\phi$. The efficiency shows a maximum value of $1/e$, i.e. about 37%. At this point of maximum efficiency the ablated volume per pulse reads:

$$\Delta V_{Pulse} = \pi \cdot w_0^2 \cdot \delta \tag{3}$$

From this one can calculate the maximum removal rate per average power which reads for a top hat beam:

$$\frac{\dot{V}_{max}}{P_{av}} = \eta_{max} \cdot \frac{\delta}{\phi_{th}} = \frac{1}{e} \cdot \frac{\delta}{\phi_{th}} \tag{4}$$

The removal rate finally depends on the energy penetration depth $\delta$ and the threshold fluence $\phi_{th}$.

Similar calculations have been done for a Gaussian shaped beam as emitted by most ultra short pulsed systems (Neuenschwander et al. (2012), Neuenschwander et al (2010), Raciukaitis et al. (2009)). Again a maximum removal rate per average power (ablation efficiency) is observed:

$$\frac{\dot{V}_{max}}{P_{av}} = \frac{2}{e^2} \cdot \frac{\delta}{\phi_{th}} \tag{5}$$

The ablated volume per pulse at this optimum point is again given by (3) i.e. this maximum efficiency is again obtained at a corresponding fluence. It has to be pointed out that the maximum value of the removal rate (5) is only obtained at this optimum point. A general expression for the removal rate of a Gaussian beam is also developed by Neuenschwander et al. (2010) and Raciukaitis et al. (2009) and reads:

$$\dot{V} = \frac{1}{4} \cdot \pi \cdot w_0^2 \cdot \delta \cdot f \cdot \ln^2\left(\frac{\phi}{\phi_{th}}\right) \tag{6}$$

or written only in terms of the applied fluence

$$\frac{\dot{V}}{P_{av}} = \frac{1}{2} \frac{\delta}{\phi} \cdot \ln^2\left(\frac{\phi}{\phi_{th}}\right) \tag{7}$$

All these considerations clearly show that the ablation process can be optimized. With the first derivation of (7) it is possible to calculate the threshold fluence:

$$\phi_{th} = \frac{1}{e^2} \phi_{opt} \tag{8}$$

Out of equation (8) the maximum removal rate per average power (5) then reduces to:

$$\frac{\dot{V}_{max}}{P_{av}} = 2 \frac{\delta}{\phi_{opt}} \tag{9}$$

With (8) and (9) it is possible to calculate the threshold fluence $\phi_{th}$ and energy penetration depth $\delta$ when the maximum ablation rate per average power and the corresponding optimal fluence are known.

For metals and pulses longer than 10 ps the threshold fluence begins to increase as shown by Schmid et al. (2011), Jaeggi et al. (2011), Neuenschwander et al. (2011), Nolte et al. (1997). But beside the threshold fluence also the penetration depth $\delta$ has an influence onto the maximum volume ablation rate. For pulse durations in the range from 10 ps to 50 ps the value of $\delta$ decreases with increasing pulse duration (Schmid et al. (2011), Jaeggi et al. (2011), Neuenschwander et al. (2011), Nolte et al. (1997)). Therefore the maximum removal rate in general drops significantly down when the pulse duration is raised. The situation changes for shorter pulses. From Dausinger et al. (2003) one expects that the threshold fluence will rest constant when the pulse duration becomes shorter than about 10 ps. If these pulses would lead to higher ablation rates this could only be caused by a higher penetration depth $\delta$ for shorter pulses.

Due to incubation effects the threshold fluence also strongly depends on the number of pulses applied, which is described for metals by Schmid et al. (2011), Jaeggi et al. (2011), Neuenschwander et al. (2012), Jee et al. (1988) and Mannion et al. (2004). Additionally it was found that also the energy penetration depth shows an incubation effect of the same kind. The maximum removal rate may therefore also strongly depend on the number of pulses applied; more details are given in Schmid et al. (2011), Jaeggi et al. (2011), Neuenschwander et al. (2011), Neuenschwander et al. (2012).

### 2.2. Modeling

All experimental data of the removal rate as a function of the applied fluence were fitted with the logarithmic ablation law (7) to get the threshold fluence $\phi_{th}$ and energy penetration depth $\delta$. But in some measurements the ablation rates don't correspond very well with the model (see Fig. (a)). In additional experiments with single pulses it can be shown that sometimes the ablation depth can be described with two or more logarithmic regimes as e.g. seen in Fig. (b). But a 2 threshold model can only be applied if two thresholds are detected in experiments with single craters. As these experiments are very time-consuming they are often not practicable. More time effective is the method with ablated squares where the threshold fluence $\phi_{th}$ and energy penetration depth $\delta$ are determined from the maximum removal rate per average power following (7)-(9). Beside the least square fit of (7) to the experimental data the maximum can also be found by a parabolic fit to the data points around it. Out of this set of the maximal removal rate power and corresponding optimal fluence the threshold fluence $\phi_{th}$ and energy penetration depth $\delta$ can be calculated with (8) and (9). The comparison between the model fit and the calculated model with the values for $\phi_{th}$ and $\delta$ from the parabolic fit is shown in Fig. (a). The parabolic fit can represent the optimum very well but deviates significantly at higher fluences.



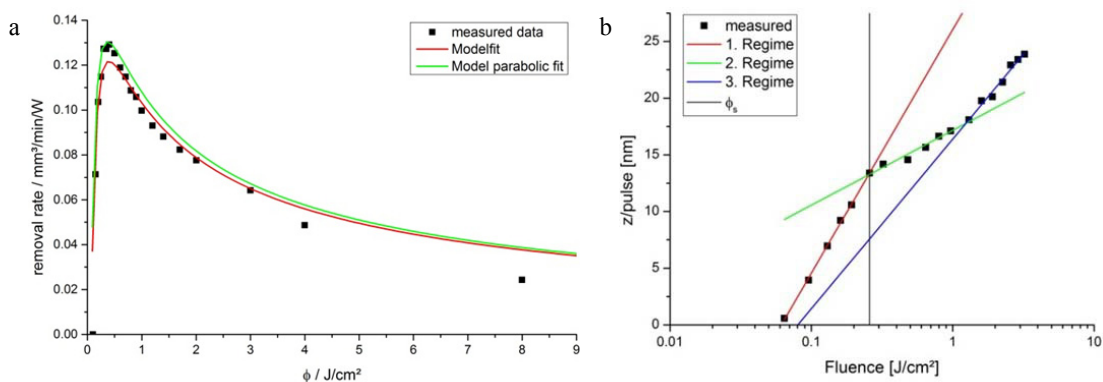Fig. 1. (a) Removal rate for stainless steel 1.4301; (b) Ablation depth with 256 single pulses.

## 3. Experimental Set-Up

The radiation of the used laser source was guided via a $\lambda$/4-plate (to generate a circular polarized beam) and folding mirrors through a beam expander into a galvo scanning head where it was focused by an f-theta objective onto the target. For the experiments three different laser systems were used:

The experiments for 10 ps and 50 ps were performed with a DUETTO$^{TM}$ (Time Bandwidth Products, Switzerland) ps-laser system working at a wavelength of 1064 nm with pulse duration of about 10 ps. By introducing a corresponding etalon into the master oscillator the pulse duration was raised up to 50 ps. The pulse duration was measured with an autocorrelator measurement whenever the etalon was changed.

For the longest pulse duration a Helios 1062-5-50 (Coherent) was used. It has pulse durations between 500 and 700ps. Here it worked at 20 kHz repetition going with pulse duration of 520ps.

For all systems the beam quality factor $M^2$ was better than 1.3. With all laser systems hatched squares with a side length of 1 mm were machined into the investigated materials with a hatch distance of near the half of the spot radius. For better comparability, pulse repetition rate and focus radius should be kept approximately equal. The experiments with DUETTO (10, 50 ps) were done at 50 kHz and a focus radius of approximately 18 µm. The squares were machined with a hatch distance of 9 µm and a scan speed of 450 mm/s. Because of the suggested pulse duration Helios-system works only at 20 kHz with a spot radius of 15.3 µm. The squares were machined with a hatch distance of 8µm and a scan speed of 160 mm/s. The hatch angle was turned by 10° from slice to slice. This procedure was repeated 5 times to obtain a measurable depth of the squares.

For each pulse duration and material a series of squares with different average powers i.e. fluences were machined. On the one hand the depth of the ablated squares was measured with a white light interferometer smartWLI-extended from GBS mbH. On the other hand the absolute machining time was calculated from the marking speed, the side length, the hatch distance, the number of slices and the number of repeats. From this the removal rate could be calculated by dividing the ablated volume by the machining time and the average power. The threshold fluence and the energy penetration depth were then deduced via a least square fit as described in the previous section. The machined squares were additionally analyzed under an optical microscope to analyze the machining quality.

## 4. Materials

All experiments were done on steel grades which are mainly used in the automotive industry. All common types of steel should be investigated. The steel grades DP-K are dual-phase steels. This steels offer a combination of high strength, low yield point and good cold formability due to their microstructure. The microstructure consists predominantly of a soft ferrite matrix, in which a second, hard, mainly martensitic phase is embedded. The Ferrite content is up to 90%. DP-K 60/98 has minimum yield strength of 600 MPa, a minimum tensile strength of 980 MPa. DP-K 45/78 has minimum yield strength of 450 MPa and a minimum tensile strength of 780 MPa. CP-W 800 is a complex-phase steel with strength of 800 MPa. Due to the chemical composition and a specific hot-rolling process this steel grade has a very fine microstructure. This complex structure is responsible for the material properties. HX 340 LAD is a high strength low alloy steel with a tensile strength of 410 – 510 MPa and yield strength of 340 – 420 MPa. RA-K 40/70, a retained-austenite steel, is a modern multi-phase steel characterized by the "TRIP" effect when worked. The microstructure consists mainly of a ferritic-bainitic matrix, in which retained-austenite is stored. The ferrite content including bainitic ferrite is up to 90 %, martensitic components can exist. It has a yield strength of 410 – 510 MPa, a minimum tensile strength of 690 MPa.

Manganese-boron steels MBW are quenched and tempered steels. The underlying material concepts in this family of steels exhibit a selected and matched chemical composition that enables curing (hot forming). This ferritic structure which exists in as-received condition is converted into a purely martensitic structure in the process. Thanks to this process MBW 1500, for example, can increase its minimum yield strength from 550 MPa in as-received condition to 1500 MPa. MBW 1500 is investigated in as-received condition. MBW 1900 could also be examined a typical curing process (Banik (2008)). The chemical composition for all of those steel grades can be looked up on http://incar.thyssenkrupp.com/7_01_000_Werkstoffe.html?lang=de.
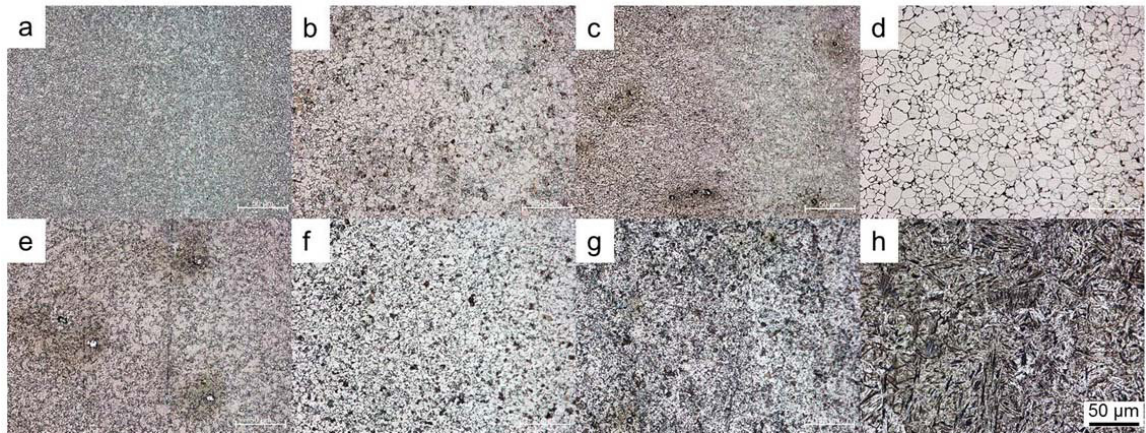
Fig. 2. Microstructure of selected steel grades; (a) DP-K 60/98; (b) DP-K 45/78; (c) CP-W 800; (d) HX340LAD; (e) RA-K 40/70; (f) MBW1500; (g) MBW 1900; (h) MBW 1900 cured.

1.3343 is a high-speed steel for cutting tools and cold forming tools. A maximal hardness of 65 HRC is possible. Steel 1.4301 was used as reference material. Fig. 2 shows the microstructure of the steels after etching with Nital.

## 5. Results

The threshold fluence $\phi_{th}$ and the energy penetration depth $\delta$ were deduced in two different ways: Firstly by a least square fit with (7) to the experimental deduced removal rates per average power. Secondly by deducing the optimum fluence and the maximum removal rate per average power with a parabolic least square fit to the experimental data fit around maximum point. From both values the threshold fluence and the energy penetration depth were calculated following (8) and (9).

For 520 ps the least square fit of the 1 threshold model fits better to the measured data. At this pulse duration we get the smallest removal rate. Due to this the ablation depth of these squares is very low and the evaluation becomes difficult. But raising the number of slices for 520 ps leads to a change of the ablation process and the machining quality. This effect is shown in Fig. 3 for 10 ps and two different number of slices. Fig 3 (a) shows the machining quality for 30 slices. It shows only small areas with craters. Raising the number to 62 the machining quality worsens. Fig 3 (b) shows the machining quality for 62 slices. Areas with craters are much bigger than for 30 slices.
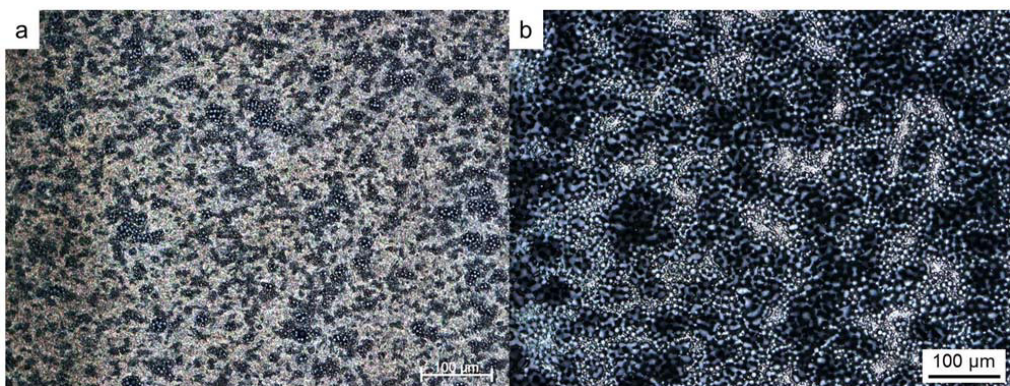


Fig. 3. Influence of the number of slices for 10 ps on MBW1500: (a) 30 slices; (b) 62 slices.

### 5.1. Pulse duration 10 ps

The deduced threshold fluences, energy penetration depths and corresponding maximum removal rates are summarized for 10 ps and all steel grades in Table 1. There are only slight differences observed. The maximum removal rate for all steel grades is similar except for 1.3343 where it is significantly lower. As also the removal rate for cured state is even lower than the initial state this suggests that the microstructure could have an influence but it is not very pronounced. In general the model fits very well to the measured data for the initial state. In hardened state there is a sharp drop in the removal rate per average power for fluences significantly higher than the optimum one leading to differences between the model and the measured data.

Table 1. Threshold fluence, energy penetration depth and maximum removal rate for ablation with 10 ps.

| Steel grade | $\phi_{th}$ model fit | $\phi_{th}$ parabolic | $\delta$ model fit | $\delta$ parabolic | $\dot{V}/P_{av}$ model fit | $\dot{V}/P_{av}$ parabolic |
|---|---|---|---|---|---|---|
| DP-K 60/98 | 0.0521 | 0.0400 | 3.93 | 3.17 | 0.122 | 0.129 |
| DP-K 45/78 | 0.0543 | 0.0375 | 4.10 | 2.98 | 0.123 | 0.129 |
| CP-W 800 | 0.0452 | 0.0404 | 3.47 | 3.19 | 0.125 | 0.128 |
| HX340LAD | 0.0527 | 0.0446 | 3.89 | 3.46 | 0.120 | 0.126 |
| RA-K 40/70 | 0.0555 | 0.0517 | 4.14 | 4.10 | 0.121 | 0.129 |
| MBW 1500 | 0.0567 | 0.0492 | 4.32 | 3.94 | 0.124 | 0.130 |
| MBW 1900 | 0.0456 | 0.0446 | 3.59 | 3.67 | 0.128 | 0.134 |
| MBW 1900 cured | 0.0544 | 0.0449 | 4.18 | 3.64 | 0.125 | 0.132 |
| 1.3343 | 0.0637 | 0.0498 | 4.38 | 3.64 | 0.112 | 0.119 |
| 1.3343 hardened | 0.0643 | 0.0559 | 4.17 | 4.06 | 0.105 | 0.118 |
| 1.4301 | 0.0535 | 0.0498 | 4.01 | 4.00 | 0.122 | 0.130 |

MBW1900 implies an influence of the microstructure, too. Even the removal rate for cured and initial state do not significantly differ, different data for $\phi_{th}$ and $\delta$ are obtained for the model and parabolic fit as illustrated in Table 1. All other steels have quite similar removal rates and only small differences in $\phi_{th}$ and $\delta$ also they may have some differences in the in microstructure as e.g. the steel grades DP-K (see Fig. 2 (a) + (b)). Therefore additional investigations are needed to clarify and quantify the influence of the microstructure.

Also the machining quality was examined. With the optimal fluence a good surface quality was achieved in all grades of steel as e.g. shown for MBW 1900 cured and initial state (Fig. 4 (a) + (e)). For higher fluences steel grades differs in their surface quality.
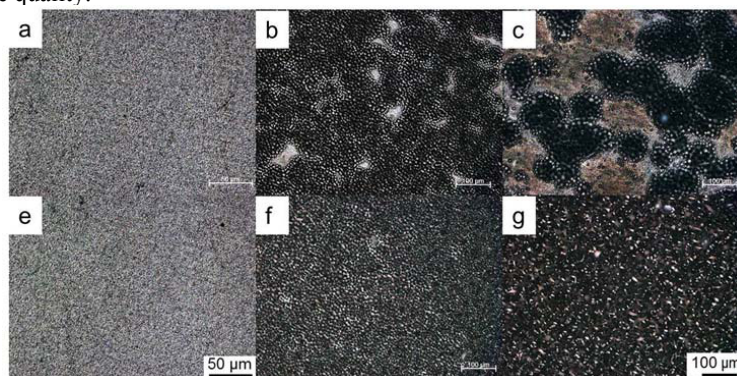


Fig. 4. Machining quality for 10 ps on MBW1900 cured (a)-(c); MBW1900 (e)-(g): (a) + (e) 0.324 J/cm²; (b) + (f) 3.23 J/cm²; (c) + (g) 10.8 J/cm².

For all steel grades crater formation starts local at certain fluences and normally continues until the whole ablated area is covered (Fig. 4(b) and (f)). After that the craters become bigger and the surface rougher as shown in Fig. 4 (f) and (g). But for some steels the crater formation is only spread until a certain fluence is reached (Fig. 4 (b)). For higher fluences the fraction of the area covered by craters is significantly reduced (Fig 4 (c)). This reduction in the covered surface was observed for DP-K 60/98, CP-W 800 and MBW 1900 cured when the fluence was raised from around 3 J/cm² to above 10J/cm². In contrast for MBW 1900 in its initial state and DP-K 45/78 the whole ablated area rests covered by craters at high fluences.

## 5.2. Pulse duration 50 ps

The deduced threshold fluences, energy penetration depths and corresponding maximum removal rates are summarized for 50 ps and all steel grades in Table 2. Some differences between the steel grades are observed. The maximum removal rate for all steel grades is similar except for the higher alloyed steels 1.3343 and 1.4301 showing an about 25% lower removal rate. Again there are some differences in $\phi$th and $\delta$ between steels in initial state and cured/hardened implying that the microstructure could have an influence.

Table 2. Threshold fluence, energy penetration depth and maximum removal rate for ablation with 50 ps.

| Steel grade | $\phi_{th}$ model fit | $\phi_{th}$ parabolic | $\delta$ model fit | $\delta$ parabolic | $\dot{V}/P_{av}$ model fit | $\dot{V}/P_{av}$ parabolic |
|---|---|---|---|---|---|---|
| DP-K 60/98 | 0.0643 | 0.0633 | 1.72 | 1.74 | 0.043 | 0.045 |
| DP-K 45/78 | 0.0639 | 0.0575 | 1.68 | 1.60 | 0.043 | 0.045 |
| CP-W 800 | 0.0666 | 0.0607 | 1.71 | 1.61 | 0.042 | 0.043 |
| HX340LAD | 0.0602 | 0.0604 | 1.61 | 1.75 | 0.043 | 0.047 |
| RA-K 40/70 | 0.0772 | 0.0593 | 1.90 | 1.49 | 0.040 | 0.041 |
| MBW 1500 | 0.0662 | 0.0649 | 1.73 | 1.74 | 0.042 | 0.044 |
| MBW 1900 | 0.0656 | 0.0603 | 1.72 | 1.69 | 0.043 | 0.045 |
| MBW 1900 cured | 0.0718 | 0.0754 | 1.87 | 2.02 | 0.042 | 0.044 |
| 1.3343 | 0.1052 | 0.0753 | 2.14 | 1.60 | 0.033 | 0.034 |
| 1.3343 hardened | 0.1575 | 0.1480 | 3.12 | 2.97 | 0.032 | 0.033 |
| 1.4301 | 0.0917 | 0.1244 | 1.94 | 2.64 | 0.034 | 0.034 |

In contrast to 10 ps all steel grades show crater formation over the whole area. At the optimal fluence the surface quality is still quite good (Fig. 5(a) + (e)) whereas for higher fluences thermal discoloration and melting occur (Fig. 5(b) + (f)). A further increase of the fluence leads to crater formation as shown in Fig. 5(c) + (d).
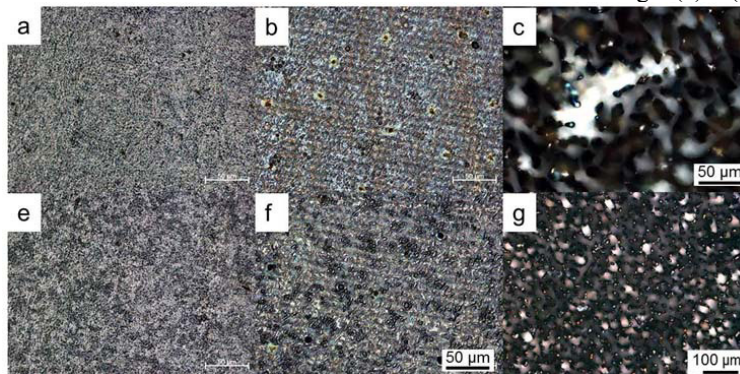


Fig. 5. Machining quality for 50 ps on MBW1900 cured (a)-(c); MBW1900 (e)-(g): (a) + (e) 0.5 J/cm²; (b) + (f) 1.6 J/cm²; (c) + (g) 10.45 J/cm².

## 5.3. Pulse duration 520 ps

The deduced threshold fluences, energy penetration depths and corresponding maximum removal rates are summarized for 520 ps and all steel grades in Table 3. Because of the low ablation rate only the least square fit with the model was performed. Even the model function (7) did not fit very well (due to the strong thermal influence) it was possible to deduce the threshold fluence and the energy penetration depth. Also here only small differences of these values and quiet similar maximum removal rates were observed for all steel grades except for 1.3343 initial state and 1.4301 where both values are significantly lower.

Table 3. Threshold fluence, energy penetration depth and maximum  removal rate for ablation with 520 ps.

| Steel grade | $\phi_{th}$ model fit | $\delta$ model fit | $\dot{V}/P_{av}$ model fit |
|---|---|---|---|
| DP-K 60/98 | 0.6150 | 2.36 | 0.0062 |
| DP-K 45/78 | 0.5182 | 2.33 | 0.0073 |
| CP-W 800 | 0.7039 | 2.85 | 0.0066 |
| HX340LAD | 0.7509 | 3.21 | 0.0069 |
| RA-K 40/70 | 0.7314 | 3.27 | 0.0073 |
| MBW 1500 | 0.7656 | 3.27 | 0.0069 |
| MBW 1900 | 0.6741 | 2.90 | 0.0070 |
| MBW 1900 cured | 0.6628 | 2.86 | 0.0070 |
| 1.3343 | 0.4498 | 1.74 | 0.0063 |
| 1.3343 hardened | 0.6064 | 2.46 | 0.0066 |
| 1.4301 | 0.4371 | 2.08 | 0.0077 |

Melting effects and boarders become clearly visible also for low fluences and they increase with increasing fluence. Thermal discoloring occurs at a certain fluences and the surface quality is reduced compared to shorter pulse durations as shown in fig. 6.
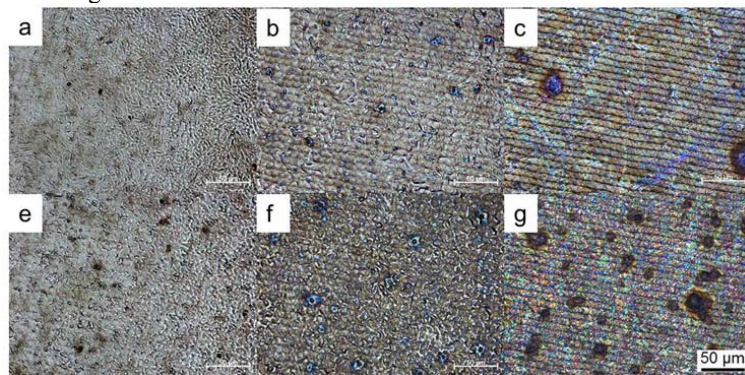


Fig. 6. Machining quality for 520 ps on MBW1900 cured (a)-(c); MBW1900 (e)-(g): (a) + (e) 0.5 J/cm²; (b) + (f) 1.6 J/cm²; (c) + (g) 10.45 J/cm².

## 6. Conclusion

With a few exceptions all tested steel grades show similar values for the threshold fluence and the energy penetration depth, resulting in also similar maximum removal rates, at all investigated pulse durations of 10ps, 50ps and 520ps. However, some differences have been observed e.g. between the initial and the hardened/cured state. It is expected that they could be caused by the microstructure of the steel but future experiments are needed to confirm this assumption.

For short pulse durations the surface quality was the most obvious difference when machining the different steel grades. This difference disappeared for longer pulse duration due of a bigger influence of thermal effects onto the ablation process. Additionally it was found that also the number of slices affects the machining quality.

## References

Chichkov, B. N., Momma, C., Nolte, S., von Alvensleben, F., Tünnermann A., 1996. Femtosecond, picosecond and nanosecond laser ablation of solids. Appl. Phys. A 63, 109.

Breitling, Detlef, Ruf, Andreas, Dausinger, Friedrich, 2004. Fundamental aspects in machining of metals with short and ultrashort laser pulses. Proc. SPIE 5339, 49-63.

Dausinger, Friedrich, Hügel, Helmut, Konov, Vitali, 2003. Micro-machining with ultrashort laser pulses: From basic understanding to technical applications. Proc. SPIE Vol. 5147, 106-115.

Meijer, J., Du, K., Gillner, A., Hoffmann, D., Kovalenko, V. S., Masuzawa, T., Ostendorf, A., Poprawe,A., Schulz, W., 2002. Laser Machining by Short and Ultrashort Pulses – State of the Art. Annals of the CIRP, 51/2

Pierrot, S., Saby, J., Cocquelin, B., Salin, F., 2011. High-Power all Fiber Picosecond Sources from IR to UV. Proc. of SPIE Vol. 7914, paper 79140Q

Kanzelmeyer, S., Sayinc, H., Theeg, T., Frede, M., Neumann, J., Kracht, D., 2011. All-fiber based amplification of 40 ps pulses from a gain-switched laser diode. Proc. of SPIE Vol. 7914, paper 191411

Schmid, M., Neuenschwander, B., Romano, V., Jaeggi, B., Hunziker, U., 2011. Processing of metals with ps-laser pulses in the range between 10ps and 100ps. Proc. of SPIE Vol. 7920, paper 792009.

Jaeggi, B., Neuenschwander, B., Schmid, M., Muralt, M., Zuercher, J., Hunziker, U., 2011. Influence of the Pulse Duration in the ps-Regime on the Ablation Efficiency of Metals. Physics Procedia 12, 164-171.

Neuenschwander, B., Jaeggi, B., Schmid, M., Hunziker, U., Luescher, B., Nocera, C., 2011. Processing of industrially relevant non metals with laser pulses in the range between 10 ps and 50 ps. ICALEO 2011, Paper M103

Sallé, B., Gobert, O., Meynadier, P., Petite, G., Semerok, A., 1999. Femtosecond and picosecond laser microablation: ablation efficiency and laser microplasma expansion. Appl. Phys. A 69[Suppl.], 382 – 383

Le Harzic, R., Breitling, D., Weikert, M., Sommer, S., Föhl, C., Valette, S., Donnet, C., Audouard, E., Dausinger, F., 2005. Pulse width and energy influence on laser micromachining of metals in a range of 100 fs to 5 ps. Appl. Surf. Science 249, 322-331

Lopez, J., Lidolff, A., Delaigue, M., Hönninger, C., Ricaud, S., Mottay, E., 2011. Ultrafast Laser with high Energy and high average power for Industrial Micromachining: Comparison ps-fs. ICALEO 2011, Paper 401

Russbueldt, P., Mans, T., Weitenberg, J., Hoffmann, H.-D., Poprawe, R., 2010. Compact diode-pumped 1.1 kW Yb:YAG Innoslab femtosecond amplifier. Opt. Lett. 35, 4169-4171

Russbueldt, P., Mans, T., Hoffmann, H.-D., Poprawe, R., 2011. 1100 W Yb:YAG femtosecond Innoslab amplifier. Proc. of SPIE, 7912

Lauer, B., Neuenschwander, B., Jäggi, B., Schmid, M., 2013. From fs – ns: Influence of the pulse duration onto the material removal rate and machining quality for metals. ICALEO 2013, Paper M309.

Steel grades: http://incar.thyssenkrupp.com/7_01_000_Werkstoffe.html?lang=de, April 2014.

Momma, C., Chichkov, B.N., Nolte, S., van Alvensleben, F., Tünnermann, A., Welling, H., Wellegehausen, B., 1996. Short-pulse laser ablation of solid targets. Opt. Comm. 129, 134-142.

Momma, C., Nolte, S., Chichkov, B.N., van Alvensleben, F., Tünnermann, A. , 1997. Precise laser ablation with ultrashort pulses. Appl. Surf. Science 109/110, 15-19

Nolte, S., Momma, C., Jacobs, H., Tünnermann, A., Chichkov, B.N., Wellegehausen, B., Welling, H., 1997. Ablation of metals by ultrashort laser pulses. J. Opt. Soc. Am. B, Vol. 14, No. 10.

Anisimov, S.I., Rethfeld, B., 1997. On the theory of ultrashort laser pulse interaction with a metal. Proc. SPIE 3093, 192-203

Christensen, B.H., Vestentoft, K., Balling, P., 2007. Short-pulse ablation rates and the two-temperature model. Appl. Surf. Science 253, 6347-6352

Mannion, P., Magee, J., Coyne, E., O'Conner, G.M., 2002. Ablation Thresholds in ultrafast laser micro-machining of common metals in air. Proc. of SPIE vol. 4876, 470-478

Neuenschwander, B., et al., 2012. Optimization of the volume ablation rate for metals at different laser pulse-durations from ps to fs. Proc. of SPIE vol. 8243, 824307-1

Neuenschwander, B., Bucher, G., Nussbaum, C., Joss, B., Muralt, M., Hunziker U., et al., 2010. Processing of dielectric materials and metals with ps-laserpulses: results, strategies limitations and needs. Proceedings of SPIE vol. 7584.

Raciukaitis, G., Brikas, M., Gecys, P., Voisiat, B., Gedvilas, M., 2009. Use of High Repetition Rate and High Power Lasers in Microfabrication: How to keep Efficiency High? JLMN Journal of Laser Micro/Nanoengineering, Vol. 4 (3), 186-191

Jee, Y., Becker M.F., Walser, R.M., 1988. Laser-induced damage on single-crystal metal surfaces. J. Opt. Soc. Am. B5.

Mannion, P.T., Magee, J., Coyne, E., O'Connor, G.M., Glynn, T.J., 2004. The effect of damage accumulation behavior on ablation thresholds and damage morphology in ultrafast laser micro-machining of common metals in air. Appl. Surface Science 233, 275 – 287

Banik, J., Flehmig, T., Hoffmann, O., Hinz, M., Lenze, F.-J., Osburg, B., Patberg, L., Sikora, S., 2008. Neue Werkstoff- und Technologieentwicklungen für modernen Karosseriebau mit Stahl. Karosseriefertigung im Spannungsfeld von Globalisierung Kosteneffizienz und Emissionsschutz; CBC 2008; 5.Ccar Body Colloquium.